



Determining Active Agents, Stability, and Mechanism of Diazinon Degradation by Magnetic Copper Ferrite Nanoparticles and Potassium Hydrogen Monopersulfate in the Presence of Ozone in Aqueous Solutions

Seyed Jamshid Moosavi¹, Abdolrahim Pazira¹, Tayebeh Tabatabaie^{1,*}, Neematollah Jaafarzadeh^{2,1} and Sahand Jorfi^{3,1}

¹Department of Environment, Bushehr Branch, Islamic Azad University, Bushehr, Iran

²Toxicology Research Center, Ahvaz Jundishapur University of Medical Sciences, Ahvaz, Iran

³Department of Environmental Health Engineering, Ahvaz Jundishapur University of Medical Sciences, Ahvaz, Iran

*Corresponding author: Department of Environment, Bushehr Branch, Islamic Azad University, Bushehr, Iran. Email: tabatabaie@iaubushehr.ac.ir

Received 2021 May 31; Revised 2021 October 09; Accepted 2021 October 26.

Abstract

According to the results obtained thus far, ozone/magnetic copper ferrite nanoparticles (CuFe₂O₄ MNPs)/potassium hydrogen monopersulfate (KMPS) is capable of totally degrading 20 mg/L diazinon (DZN) with 6 mg/L ozone, 0.6 g/L KMPS, and 0.1 g/L MNPs at pH = 7 in 20 min. The experiments showed that the concentrations of KMPS and MNPs were more effective than ozone on the system efficiency. Moreover, high concentrations of KMPS and MNPs were not very effective in DZN degradation. Furthermore, the degradation efficiencies of diazinon at pHs 3, 4, 5, 6, 7, 8, 9, and 10 were 94%, 95.35%, 97.45%, 98.15%, 99.2%, 99.3%, 99.3%, and 100%, respectively. The pH of the solution was effective on the system so that in the range of 7 - 10, the system had high efficiency. Even within the range of 3 - 6, the pH had not been so plummeted, resulting in a high percentage of DZN degradation. Besides, MNPs could be utilized in the system for up to five cycles without any loss of catalytic activity. The degradation efficiency of diazinon was 99.2% in the first use and 92.1% in the fifth use. Also, the process efficiency was assessed in four real environments showing that agricultural drainage and urban wastewater with the degradation percentages of 79.1% and 77.3%, respectively, were better treated than the urban and river water with the percentages of 93% and 88.4%, respectively. With the determination of active agents in the reaction using the scavenging agents, it was recognized that sulfate radicals, hydroxyl radicals, superoxide, and singlet oxygen contributed to DZN degradation. By the way, ozone was advantageous to both singlet oxygen and superoxide in the degradation of diazinon.

Keywords: Advanced Oxidation Processes, Magnetic Nanoparticles, Degradation, Diazinon

1. Background

The increasing development of industries, followed by the release of industrial wastewater into the environment, has raised many concerns about surface and groundwater pollution and environmental destruction. The release of toxic substances into the environment may adversely affect humans and other living organisms. Contamination because of the accumulation of toxic substances in the soil causes diseases that damage the growth and health of both animals and humans. One of the sources of environmental pollution is persistent organic compounds in the wastewater of chemical industries and agricultural effluents. The presence of such compounds in aqueous media changes the chemical quality (chemical oxygen demand, pH, alkalinity, acidity, dissolved oxygen, etc.) and physical quality (color, temperature, odor, viscosity, turbidity, etc.) of water. Among various pollutants in aquatic environments are aromatic compounds with high stability, attracting the most attention.

Nowadays, the increasing need for food has given rise to the development of agriculture, followed by the upsurge in the use of water and chemical products related to agriculture. Predictably, along with the increase of population, the need for food has also increased, and to accelerate the production and protection of plant products, the use of pesticides and herbicides has become unavoidable.

Agricultural pests are among the essential factors deterring the growth of plants. One of the most common

ways to avoid these factors is to use chemical pesticides like diazinon (DZN). As a phosphorus compound employed in the soil and on the aerial parts of the plants, DZN has been utilized since 1977 to fight rice stem borers in the north of Iran. This pesticide was of the highest usage (over 10% of all) in Iran in 2010 (1). Diazinon is applied to ward off garden pests, domestic insects, mosquitoes, and flies in stables (2). It may be used in spraying of the garden parks, as well (3). Although such materials have been proven valuable in increasing foodstuff and victuals, their wastes yet found in groundwater and rivers have yielded scores of harm to the ecosystem and human beings. Thus, investigators are searching for ways to curb such agricultural chemicals since these compounds are resistant to biotic degradation and retained in the ecosystem for a long time to have irremediable effects on human health at low concentrations (4-8). Among the treatment methods, though inexpensive and eco-friendly, biological treatment cannot degrade pesticides entirely due to their toxicity to microorganisms (9).

The conventional procedures for treating sewage and degradation of toxins and biodegradable materials are often inefficient. Meanwhile, persistent organic pollutants (POPs), herbicides, pesticides, and dyestuffs are environmentally significant. In the recent 30 years, various chemical, photochemical, and electrochemical methods have been developed to resolve this setback. Asgari et al. used catalytic ozonation for degradation of diazinon. For this purpose, manganese oxide nanoparticles, carbon nanotubes, and graphite under the influence of ozone in an aqueous medium have been used in diazinon degradation (10). Khoiriah et al. used the photocatalytic method with TiO_2 catalyst to degrade diazinon (11). Molla Mahmoudi et al. electrochemically removed diazinon by applying graphite anodes (12). Heidari et al. used the electro-Fenton method to degrade diazinon, where they employed the potential of the electro-Fenton process with iron anodes (13). In a study, Farhadi et al. used zero-capacity iron nanoparticles on chitosan natural polymer (CS/nZVI) to remove diazinon (14). Advanced oxidation methods include techniques based on the generation of hydroxyl radical (OH^\bullet) in the environment. As a strong oxidant, OH^\bullet can degrade organic compounds and aromatic rings of refractory compounds. Advanced oxidation processes (AOPs) are introduced by Glaze et al. (15) as follows: "The processes at ambient temperature and under normal pressure to generate high-activity radicals (especially, OH^\bullet radicals)." It has been established that these processes could not generate toxic compounds during the reaction. Also, the degrada-

tion of all organic matters may be rendered through AOPs (16-18).

As known, OH^\bullet radicals have the highest efficiency in the oxidation of organic compounds because of the high oxidation potential, reduction of radicals, and the non-selectivity of the compounds oxidized by them. The redox potential E^0 for the hydroxyl radical equals 2.8 V, owing to the short lifespan of this radical, which should be locally produced and consumed. The preparation of OH^\bullet radicals at high concentrations before treatment operation is not recommended (19, 20). Some AOPs include the Fenton process, photocatalysis, UV/ H_2O_2 , ozonation, proxone, oxidation, sonolysis, processes based on sulfate radicals generation, and hybrid processes. Nowadays, the AOPs based on sulfate radicals are in full swing. In these processes, sulfate radical ($\text{SO}_4^{\bullet-}$) is produced locally as the primary contributor to pollutant degradation. The sulfate radical has a redox potential of 2.5 - 3.1 V, which exceeds that of hydroxyl radical (2.7 V). Besides, the lifespan (30 - 40 ms) of this radical is longer than that of hydroxyl radical (20 ns), which affords more instances for the degradation of the pollutant (21-24).

One could employ KMPS (HSO_5^-) (25, 26) to generate these radicals. One of the common peroxygens used in Oxone salt ($\text{KHSO}_5 \cdot 0.5\text{KHSO}_4 \cdot 0.5\text{K}_2\text{SO}_4$), KMPS, is utilized to synthesize many organic substances. Since 2003 this salt has been used as a strong oxidant to degrade organic pollutants. Besides, Oxone is considered an auxiliary to chlorine pools. Recently, much attention has been paid to applying this substance in the environment, especially in the degradation of organic pollutants, with most application in treating contaminated water (16, 27-30). There are a variety of approaches in the activation of KMPS to generate sulfate radicals, including transition metals (iron, cobalt, and copper), heat, ultraviolet radiation (25, 31), and ultrasonic waves (32). Iron has received exceptional attention from investigators among the transition metals due to its high abundance in the soil and less toxicity (22, 33).

A host of research has been performed thus far for the degradation of different pollutants by sulfate radicals from among which the activation through transition metals as homogeneous and heterogeneous compounds are used time and again. Applying homogene, through of superior efficiency, is together in conjunction with an intricate recovery. Alternatively, the heterogeneous process could be along with the catalyst recovery and avoidance of transition metals (34). Combining two or more AOPs in a reactor is referred to as an advanced hybrid oxidation process such as photo-Fenton, sono-Fenton, $\text{O}_3/\text{H}_2\text{O}_2/\text{UV}$,

photo-sonolysis, sonophotocatalysis, sonolysis, ozonation, electro-Fenton, etc. The hybrid or combined processes are used for increasing efficiency, and nowadays, various combinations of AOPs concerning persistent and toxic substances are adopted (35, 36). Both ozone and KMPS can be activated as heterogeneous to generate hydroxyl and sulfate radicals, respectively. The heterogeneous catalysts are extensively utilized to activate these two oxidants. These catalysts are classified into the following groups:

- (1) Metals and metal oxides
- (2) Carbon
- (3) Composites of metals and carbon on various supports (28, 29, 37).

Thanks to high stability and catalytic recovery, metal oxides are better off amongst heterogenic catalysts and have gained the most interest in numerous reuse cycles. Although cobalt oxides play the best in activating KMPS, iron-based metal oxides have been of the most application among others. Because some iron oxides hold magnetic properties, separating them from the solution is much easier. To mention some, we recall Fe_3O_4 , $\gamma\text{-Fe}_2\text{O}_3$, and $\text{FeO}(\text{OH})$, which are widely employed in the activation of hydrogen peroxide (38, 39).

In the last years, spinels with the general formula of AB_2O_4 have been used to activate some kinds of oxidants, where A and B are alkaline earth metals or transition metals (40, 41). The element B in the formula above is, more often than not, taken to be iron, usually known as ferrite. The ferrite nanoparticles are taken up frequently as absorbents, catalysts, and photocatalysts to restrain environmental contaminations. Magnetic copper ferrite nanoparticles (CuFe_2O_4) alias MNPs are considered the most used spinels, having long occupied a significant role in the pharmaceutical and metallurgical industry, thanks to their high magnetic property, gained due attention in the AOPs for degradation of organic materials. Comprised of hematite (Fe_2O_3) and copper oxide (CuO), whence possessing both metal oxides, MNP has been the focus of attention due to its high magnetic property. Indeed, the reduction-oxidation cycle of metals may be facilitated with the presence of the oxidant so that $\text{Fe}_2^+/\text{Fe}_3^+$ and $\text{Cu}_2^+/\text{Cu}_3^+$ could be continually turned on each other during the reaction (42, 43).

Copper nanoferrite has been used as a catalyst for potassium hydrogen monopersulfate (42), persulfate ($\text{S}_2\text{O}_8^{2-}$) (44), hydrogen peroxide (40), and ozone (45). The use of a catalyst to activate two oxidants simultaneously has been less studied yet. On the other hand, the interaction of dioxidants without an activating agent should

have a synergistic effect.

In this study, performed at the Faculty of Environmental Health, Shiraz University of Medical Sciences, diazinon degradation was investigated via the production of sulfate radicals with intermediate metals heterogeneously in synthetic diazinon aqueous solution. In the case of aqueous diazinon solution, a heterogeneous process ($\text{O}_3/\text{MNPs}/\text{KMPS}$) is used. To this goal, CuFe_2O_4 metal oxide spinel activates potassium, hydrogen, monosulfate, and ozone.

2. Methods

The method used for this research is a classic and common method for optimizing a process or analyzing, the so-called “one factor at a time method” or OFAT, for short. The OFAT method is such that we change the desired variable in a particular range while assuming the other variables to be constant and then, by considering the effects of the changing variable upon the response of the process or the analysis results, the optimum value of the variable would be acquired. This approach is widely used. In situations where data are cheap and abundant, there are cases where the mental effort required to perform a complex multifactorial analysis is more than the necessary effort to obtain additional data. In this case, OFAT would be a very rational method.

2.1. Chemicals and Reactants

In this study, KMPS, tert-butyl alcohol, ethanol, and methanol for the HPLC apparatus were made available through Merck Co. Diazinon (CAS number 333-41-5) ($\text{C}_{12}\text{H}_{21}\text{N}_2\text{O}_3\text{PS}$) was provided via Sigma Aldrich Co. Water to be used in the HPLC equipment was provided through Sam Chum Co. Laboratory water supply was used for deionized water in the Laboratory of School of Environmental Health, Shiraz University of Medical Sciences.

2.2. Synthesis of CuFe_2O_4 and Its Characterization

Simultaneous precipitation of iron and copper salts was utilized to synthesize CuFe_2O_4 . In this method, copper nitrate and iron nitrate were mixed in a ratio of 1:2 and precipitated under ambient conditions via an alkaline precipitation agent (46). In this regard, 25 mL of 0.25 mM copper nitrate solution was blended with the same volume of 0.50 mM iron nitrate for 15 minutes using a magnetic stirrer. Then, the solution was precipitated through a burette dropwise using ammonium hydroxide (0.28%) until its pH reached 12.5 before exposing the dark-colored precipitate

to 80°C in the oven for one hour. The precipitate obtained was then washed several times with deionized water before being incubated in the oven at 105°C for two hours and dried. Then, the obtained sample was heated at 600°C in the oven for four hours to be calcinated (46). Field emission scanning electron microscopy (FESEM) (TESCAN Mira 3) was taken to depict the particles' morphology and sizes. X-ray diffraction (XRD) analysis was carried out for the crystallographic purposes of the nanoparticles and confirmation of substance synthesis, which was documented through an advanced D8 Bruker diffractometer with Ka-Cu radiation. Vibration saturation magnetism (VSM) was applied to evaluate the magnetic property of copper nanoferrite. The Brunauer-Emmett-Teller (BET) theory was helpful with Belsorp mini II (Japan) to measure the specific surface area, volume, and other pore dimensions. The energy-dispersive spectroscopy (EDS) was performed utilizing TESCAN Vega 3 to analyze the weight percentage of nanoparticles. A fourier transform infrared (FTIR) approach (Bruker Tensor II) was adopted for the determination of the bonds (47).

2.3. Degradation of DZN in Ozone/MNPs/KMPS System

Closed conditions were taken on to scrutinize the reaction mechanism. The 20 mg/L DZN solutions were supplied daily. The KMPS solution with a 100 mM concentration was also prepared daily. A cylindrical reactor was used to supply the ozone stock solution, and 500 mL deionized water was added to the reactor. Using an ozone generator with the power of 0.4 g/h, the ozone gas was continually sprinkled into the system through a ceramic diffuser for 30 min until the concentration reached a steady state. The concentration was repeatedly monitored using the iodometric method. It reached 3.3 ± 0.3 mM in the stock solution. To start the process, the DZN solution with a particular concentration (5 - 40 mg/L) was added into a 500 mL sealed flask together with copper nanoferrite (0 - 0.4 g/L), KMPS (0 - 1.2 g/L), and ozone (0 - 20 mg/L). The flask was put on a shaker at a 225-rpm speed at 25°C. Sodium hydroxide and sulfuric acid regulated the pH of the solution. The samples were then passed through a syringe filter with a diameter of 0.22 microns before being quenched by methanol for HPLC analysis. The parameters such as catalyst dose, pH, KMPS dose, ozone dose, and the initial concentration of the pollutant were examined.

To assess the reusing of the copper nanoferrite catalyst, MNPs were washed with deionized water following the examination of the operation parameters and then were dried and went into the test under previous condi-

tions. Furthermore, both iron ions and copper ions were measured. Additionally, the process efficiency was evaluated in the actual environment like urban water, river water, treatment plant secondary effluent, and agricultural drains. Using the TOC index, the rate of carbon mineralization was determined. To characterize the radicals, four scavengers, tert-butyl alcohol, ethanol, sodium azide, and 4-benzoquinone, were made into use, each of which decreased the active species of the oxidant as discussed in the next section. The process efficiency was examined by the following Equation 1:

$$\text{Removal efficiency (\%)} = \frac{\text{diazinon}_0 - \text{diazinon}_t}{\text{diazinon}_0} \times 100 \quad (1)$$

All the above experiments were performed in the laboratory of the Environmental Health Faculty, Shiraz University of Medical Sciences.

2.4. Measurement Methods

The high-performance liquid chromatography (HPLC) with a UV detector was used to evaluate DZN. The wavelength of 220 nm previously determined by the spectrophotometer was adopted to measure DZN. Column C18 of 150 mm height and 4.6 mm diameter containing 5-micron particles was considered the stationary phase. On the other hand, the mobile phase holding water and methanol with the proportion of 30:70 was used isocratically to separate the substance with the 0.8 mL/min flow rate. Also, 20 microliters of the sample were injected manually into the system. The wavelength of the peak time was set between 4.8 and 5.2 min while the analysis was rendered up to 10 min. The concentrations of 0.01 mg/L to 40 mg/L were injected into HPLC as standards. The calibration curve was found to have $R^2 = 0.9999$. To measure the ozone, the iodometry method was undertaken (48). The ozone concentration in the entering gas flow was determined via iodometric titration. The present study measured COD and BOD based on the standard method (49). Besides, TDS was gauged via a TDS meter (HACH). The iron and copper concentrations were obtained through an atomic absorption spectrometer. The above measurements were conducted in the Faculty of Environmental Health laboratory, Shiraz University of Medical Sciences.

3. Results and Discussion

3.1. Effects of Parameters in KMPS/MNPs/Ozone

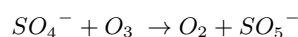
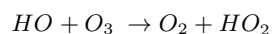
The pH of solutions is deemed as a vital parameter in AOPs. Aside from affecting the oxidation of the radicals,

it could influence the catalyst surface and accelerate the absorption of the pollutant and the oxidant on the catalyst surface (50). To realize the effect of the solution pH, the DZN removal efficiency was investigated with the conditions of 6 mg/L ozone concentration, 20 mg/L DZN concentration, 0.6 g/L KMPS, and 0.1 g/L catalyst dose for 20 min. According to the results, the highest efficiencies were attained in the neutral pH and beyond so that they were 94%, 95.35%, 97.45%, 98.15%, 99.2%, 99.3%, 99.3%, and 100% at pH = 3, 4, 5, 6, 7, 8, 9, and 10, respectively. The process was trimmed down in acidic conditions. The increase in efficiency in the alkaline and neutral pHs can be rooted in the alkaline conditions in the ozonation process tend to free radicals production, whereas KMPS approaches the degradation of non-free radicals in the alkaline conditions (51, 52). It is worth noting that the oxidation power of radicals, particularly hydroxyl radicals, decreases in the alkaline pHs. Accordingly, the oxidation power of the hydroxyl radical in the alkaline pH equals 1.8 V, while in the acidic condition, it reaches 2.8 V (53). Several studies concerning the processes based on sulfate radical guarantee that the system's effectiveness is highest in neutral conditions. On the other hand, it is observed that the process efficiency has turned down in the acidic conditions, which is caused by the presence of a host of hydrogen ions capable of neutralizing sulfate and hydroxyl radicals (Equations 2 and 3) (54, 55).

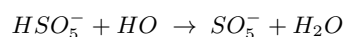
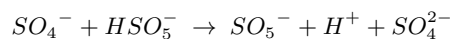


This phenomenon was observed in many studies about dyestuff and persistent organic materials in the processes based on sulfate and hydroxyl radicals (54, 56). According to the obtained results, pH = 7 was taken (47). The effects of the oxidant dose were always directly related to free radical production as the primary agent of degradation. Thus, the effect of ozone concentration was examined at pH 6, catalyst dose 0.1 g/L, KMPS 0.6 g/L, and DZN concentration 2 mg/L for 20 min. As ozone concentration increases, the process efficiency grows slightly, possibly due to more free radicals and reactive oxygen species (ROS) production. When the ozone concentration was zero (MNP/KMPS process), the efficiency was 95.3%, probably associated with the production of sulfate radicals arising from the activation of KMPS with MNPs. Adding up ozone led to a slight increment in the process efficiency. This result shows that ozone causes an increase in free radical production. Incidentally, the rise in the ozone concentration had no manifest effect on the efficiency, which might be linked with

the ozone reaction with sulfate and hydroxyl radicals, followed by the production of hydroperoxyl and KMPS, which are of lower oxidation power. The overdose of ozone concentration is not hitherto investigated in the literature, although the catalytic and direct ozonation were reported repeatedly (57).

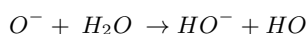
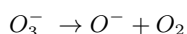
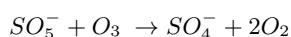
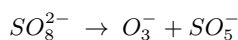
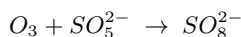


On this basis, since the reaction not including ozone with the 95% efficiency was also possible, a 6 to 8 mg/L of concentration may well enough substantiate the ozone function in the system (47). Other than ozone, the KMPS concentration may be effectually decisive in producing various oxidant species. So, the effect of KMPS dose on the process was studied under the conditions of catalyst dose 0.1 g/L, pH = 7, ozone 6 mg/L, and DZN concentration of 20 mg/L in 20 min. In the absence of KMPS (MNP/Ozone), the DZN removal efficiency approached 87%, possibly because of the catalytic degradation of ozone in the catalyst's surface. The efficiency increased by including a little KMPS (0.3 g/L) due to free radical production. Extending to 0.6 g/L of KMPS, the efficiency of the process for removal of DZN reached 95.3% (51). However, more dosage increment of KMPS towards 1.2 g/L was not conducive to an increase in the efficiency due to the reaction of the extra (or not reacted) KMPS with free radicals, yielding to the prevention of free radicals reaction with DZN (30, 47, 58).



Several investigators report the inhibitory effect of KMPS at high concentrations. Regarding dye removal, Jaafarzadeh, et al. (25) stated that the KMPS concentration at high doses might produce the inhibitory property. Madhavan et al. believe that the reaction of KMPS with these radicals is of a pretty high speed ($10^5 \text{ M}^{-1}\text{s}^{-1}$) (59, 60). The catalyst dose may mainly operate on behalf of oxidants activation as its value could make the active sites for the degradation of oxidants. Hence, the catalyst dose effect was tested at 0.6 g/L o KMPS, pH 7, 6 mg/L ozone, and 20 mg/L DZN concentration for 20 min. In the lack of MNPs (KMPS/ozone), the efficiency rate of the process for DZN removal was 96.9%. This shows that the relationship between scavengers and these two oxidants is more of a feat than the catalytic ozonation and the activation of heterogeneous KMPS. This is because ozone and KMPS are of synergic effects to the sense that ozone may operate as an activator for KMPS such that first, ozone reacts with potassium

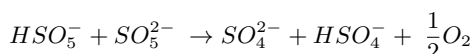
hydrogen monopersulfate ions before the production of ozonide radicals and KMPS. Then, the sulfate and hydroxyl radicals are generated as the ultimate product and the primary agent of degradation (61).



The addition of copper nanoferrite to the system led to a bit increase in the process efficiency. The increase was so that for doses of 0.5, 0.1, 0.2, 0.3, and 0.4 g/L, the DZN removal efficiencies were 97.98%, 98.6%, 96.4%, 98.6%, and 100%, respectively. As seen, the efficiency percentage grows a little along with the increase in the catalyst concentration; after the latter rises by 0.1 g/L, however, the increase of the former is not noteworthy whence a dose of 0.1 g/L could be well effective in the system (47).

3.2. Determination of Active Agents in Degradation of DZN by KMPS/MNPs/Ozone Process

As usual, chemical alcohols are employed in sulfate radical-based processes to determine active species in the degradation of pollutants. Accordingly, one of the alcohols is used to scavenge both hydroxyl and sulfate radicals, and the other is applied to scavenge hydroxyl radicals. The dissimilarity between these two scavengers indicates the rate of sulfate radical participation. On account of its fast rate of reaction with sulfate and hydroxyl radicals to scavenge them, ethanol was utilized in the present investigation (27). On the other hand, alcohol without alpha hydrogen, such as tert-butyl alcohol (TBA) with a reaction constant of $3.8 - 7.6 \times 10^8 \text{ M}^{-1}\text{s}^{-1}$, may be used for hydroxyl radicals. The reaction speed of this alcohol is 1,000 less likely relative to sulfate radicals, so one could infer the latter's participation by regarding the disparity between them (62). Aside from sulfate and hydroxyl radicals, superoxide ($O_2^{\bullet -}$) and singlet oxygen (1O_2) could be generated during ozonation. Singlet oxygen is even reported to be produced in the processes based on KMPS (63, 64).



One applies sodium azide and benzoquinone to scavenging singlet oxygen and superoxide (65, 66). Therefore, to determine active species, the four scavengers were analyzed in the four systems of KMPS/MNPs/ozone, MNPs/KMPS, MNPs/ozone, and KMPS/ozone. Figure 1a shows the inhibitory effect in the KMPS/MNPs/ozone system. As observed, the degradation of DZN in contact with ethanol was decreased, and the removal rate reached 27%. These occurrences imply the participation of sulfate and hydroxyl radicals in the degradation of DZN. In the presence of TBA, the rate of degradation was 65% in 20 min reaction time to the effect that hydroxyl radical has been of dimmer responsibility than sulfate radical though, in aqueous solutions, sulfate radical could also be transformed into hydroxyl radical. This fact is mentioned in the works of Ahmadi et al. (67), Yao et al. (68), and Zhou et al. (64).



In the presence of sodium azide (SA), the efficiency rate of the system diminished, which is a token of the singlet oxygen participation in DZN degradation. Nonetheless, SA is known as a scavenger for hydroxyl radical as well, such that its speed of reaction with hydroxyl ($1 \times 10^9 \text{ M}^{-1}\text{s}^{-1}$) is near that with singlet oxygen ($2 \times 10^9 \text{ M}^{-1}\text{s}^{-1}$) (65, 69). Hence, SA has probably been advantageous to the inhibitory effect for hydroxyl radical, too. The difference in the efficiency in the presence of TBA and SA can indicate the singlet oxygen participation in the degradation of DZN. In the company of BQ, the process efficiency has slightly weakened by which one concludes that superoxide has been effectual, not as much as the other active agents. Figure 1b indicates that KMPS/ozone performs almost the same behavior as above except that the rate of SA inhibitory effect here is more. This means that the role of singlet oxygen in DZN degradation has lessened and that the main factor responsible for the singlet oxygen production was catalytic ozonation. By activating KMPS with NaOH, Qi et al. (65) proved singlet oxygen as the primary agent in the degradation; however, the current study sheds more light on the character of ozone.

Figure 1c presents the scavengers effects in the MNPs/KMPS system. As seen, the degradation rate is almost conserved in the presence of three scavengers of TBA, SA, and BQ, which guarantees that the main factor in this system is sulfate radical. Meanwhile, decreases in the removal efficiency were observed because hydroxyl radicals may also be conducive to the degradation. The sulfate radical in the aqueous solution could be changed

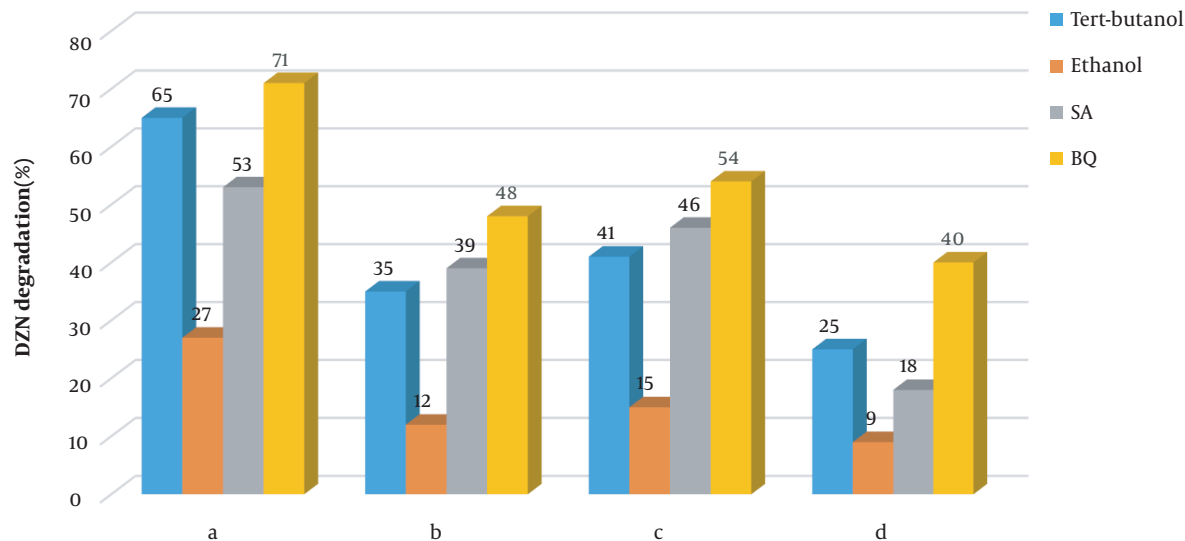


Figure 1. Effects of various scavengers on different systems (a) MNPs/ozone/KMPS; (b) ozone/KMPS; (c) MNPs/KMPS; (d) ozone/MNPs; 0.6 g/L KMPS, 0.1 g/L catalyst, 6 mg/L ozone, pH = 7

into hydroxyl radical. Last but not least, the functionality of the four scavengers could be perceived in [Figure 1d](#). Notice the much greater function of SA than TBA, owing to the proactive role of singlet oxygen. However, both BQ and, specifically, TBA were also contributing to reducing the efficiency of the process to show the role of hydroxyl radical in the system. From the discussion above, one deduces that any of the four active species plays a crucial role in the degradation of DZN. According to these results, a scheme of the process mechanism is depicted in [Figure 2](#).

3.3. Stability of Catalyst in Reusability and Actual Environments

Reusability is amongst the applied aspects of catalysts usage. To this end, as said before, the catalyst was separated from the system after the reaction and then was washed with deionized water and dried at 65°C before being reused. [Figure 3](#) illustrates the rate of DZN removal in five cycles in the conditions pH = 7, 0.6 g/L KMPS, 6 mg/L ozone, 20 mg/L DZN concentration, and 0.1 g MNPs during 20 min. As observed, no changes were taken place in the system until three catalyst cycles were used, and the efficiency of the process remained constant. Following the third cycle, the efficiency reduced a bit while the removal rate remained in good enough conditions so that during the 20 min reaction time, the removal rate was 95%. This rate reached 92.1% in the fourth cycle, which was still satisfactory. Nevertheless, this efficiency decrease may be

due to the deactivation of the catalyst surface via the by-products arising from DZN degradation, which are conglomerated during the five cycles. The catalyst restoration was done only by washing and drying at 65°C, which is a mild condition. Hence, one could acknowledge that the synthesized MNPs are very stable and reusable.

3.4. Comparing the Results with Works of Others

According to [Table 1](#), Asgari et al. used catalytic ozonation to degrade diazinon. Their study used manganese oxide nanoparticles, carbon nanotubes, and graphite under the influence of ozone in the aqueous medium. Coefficient analysis for each independent variable indicated that pH, catalyst, and reaction time have striking positive effects. On the other hand, the diazinon concentration had a significant negative effect on diazinon removal during catalytic ozonation. In this study, under conditions of pH = 10, 1.5 g/L catalyst, and 15 min reaction time, 10 mg/L diazinon was degraded with a reaction efficiency of about 90%. The mineralization rate was measured based on TOC, and a 25% rate was obtained. Also, the nanoparticle was still stable after five reaction steps (10).

Khoiriah et al. applied the photocatalytic method with TiO₂ catalyst to degrade diazinon. In this study, under conditions of pH = 5, 12 mg/L catalyst, and 30 min reaction time, 18 mg/L diazinon was degraded with a reaction efficiency of about 90%. They deduced in their study that with

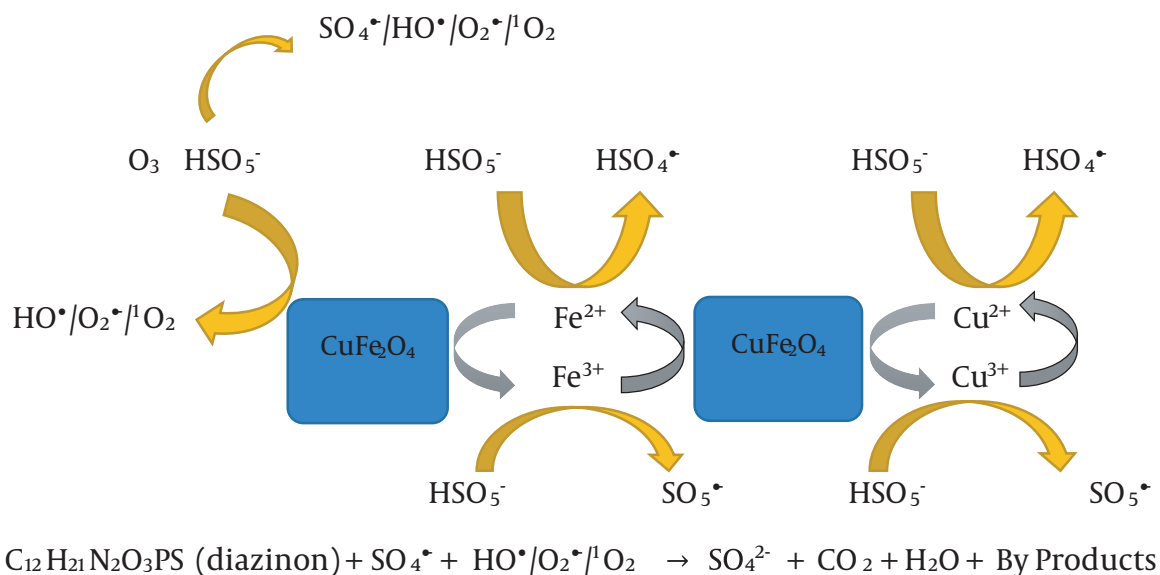


Figure 2. Mechanism of DZN degradation.

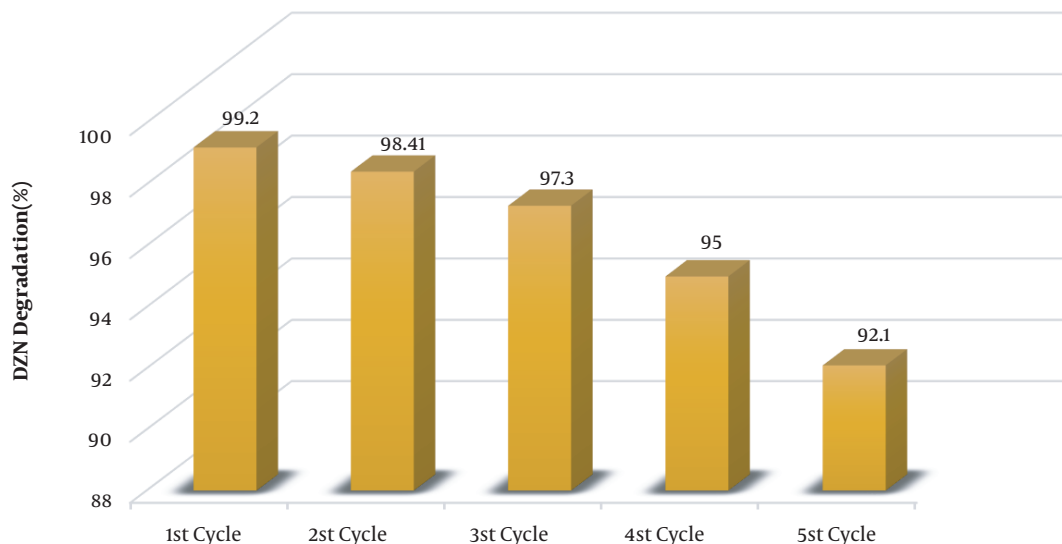


Figure 3. Five cycles in reusability of MNPs.

increasing pH and catalyst concentration, the decomposition efficiency of diazinon decreased, and also, with increasing the concentration of diazinon, the reaction efficiency declined. The reaction kinetics are in accord with the first-order reaction (ii).

Molla Mahmoudi et al. electrochemically analyzed di-

azinon and used graphite anodes in this method. Under conditions pH = 4.5, time 80 min, Na₂SO₄ concentration 1.0 g/250 cc, and electric current of 6.5 mA/cm², 80 mg/L of diazinon was degraded with an efficiency of 81.77%. The reaction efficiency decreased with increasing pH and increased with the increase in electric current. The suggested kinet-

Table 1. Comparing the Results with Works of Others

Oxidation System	Catalyst	Catalyst Dosage	Oxidizing	Reference Number
NanoMgO@CNT@Gr@O ₃	nanoMgO@CNT@Gr	1.5 g/L	Diazinon	(10)
Photocatalytic degradation	C, N-codoped TiO ₂	12 mg/L	Diazinon	(11)
Electrochemical degradation	graphite anode	6.5 mA/cm ²	Diazinon	(12)
Electro-fenton process	electro-fenton process	5.14 mA/cm ²	Diazinon	(13)
Zero valent iron supported on biopolymer chitosan	Zero valent iron	0.05 g/L	Diazinon	(14)

ics for this reaction was also of the first order. In this investigation, diazinon and COD removal efficiency diminished as diazinon concentration increased (12).

Heidari et al. accomplished the degradation of diazinon using the electro-Fenton method. In their study, the potential of the electro-Fenton process with iron anodes has been used to degrade diazinon. Besides, pH was the main parameter influencing the efficiency of the electro-Fenton process. According to the results, the efficiency of diazinon degradation increased with the increment of applied current density, reaction time, and H₂O₂ concentration, while the efficiency decreased as pH increased. The highest degradation efficiency of diazinon (100%) was obtained under optimal conditions of the studied parameters; for example, H₂O₂ concentration as 0.32 mM/l, pH = 3.0, reaction time 34.49 min, and flow rate 5.14 mA/cm². The above results inferred that the electro-Fenton process is an appropriate way to eliminate persistent organic compounds, including organophosphorus pesticides, from aqueous media (13).

In an investigation, Farhadi et al. used zero-capacity iron nanoparticles on chitosan natural polymer (CS/nZVI) to remove diazinon. In that study, the CS/nZVI composite was successfully synthesized by removing diazinon from an aqueous solution. By putting nZVI on chitosan, the stability of the nanoparticles increased. It makes the degradation more efficient and leads to a uniform distribution of nZVI. Optimization of experimental conditions such as pH, contact time, adsorbent concentration, and diazinon dose to remove diazinon was performed by CS/nZVI composite. The pseudo-first-order and pseudo-second-order models were tested, and the results indicated that adsorption is performed with the pseudo-second-order. Moreover, two isotherm models were used, including Langmuir and Freundlich. Diazinon adsorption has been shown to correlate well with the Freundlich isotherm. In general, the CS/nZVI composite has many advantages such as low cost, eco-friendliness, high performance, which is an excellent prospect in effectively removing diazinon from aqueous

media (14).

In reactions using hybrid processes, the overlap of the reaction components is significant. In this investigation, the two oxidants of ozone and potassium hydrogen monosulfate are used, deposited on nanoparticles, and degraded diazinon. The duration of 20 min to perform the reaction, the concentrations used for the oxidants, and the pH of the reaction (pH = 7, 6 mg/L ozone, 0.6 g/L KMPS, and 0.1 g/L MNPs) all indicated that the values are very appropriate and optimal. This optimality is a token of the synergistic power of the oxidants and their coordination on the nanoparticles to perform the reaction. The evidence above suggests that applying the hybrid advanced oxidation process is successful for the degradation of diazinon.

3.5. Conclusions

The function of the KMPS/MNPs/ozone process in the actual environment was investigated. To this purpose, the DZN solution was injected into the four actual environments of urban water supply, Estahban River, the urban secondary effluent, and the agricultural drainage water. The system's efficiency in deionized water turned out to be 99.2% and was employed in the control experiment. On the other hand, the efficiency in the urban water supply and Estahban River decreased to 93.05% and 88.4%, respectively, due to the high presence of water dissolved solids (Figure 4). The presence of organic matter in the Estahban River, albeit slightly, could be one of the factors reducing the process efficiency. The efficiency rate in urban secondary effluent and agricultural drainage water decreased to a greater extent: 77.3% and 79.1%, respectively. In addition to different anions scavenging the free radicals, the presence of the above-mentioned organic matter (COD = 175 mg/L for secondary effluent and COD = 98 mg/L for drainage) causes the efficiency to reduce. In other words, the organic matter in drainage and secondary effluent emulates with DZN to react with radicals. In this manner, the reaction of free radicals with the target pollutant is prevented.

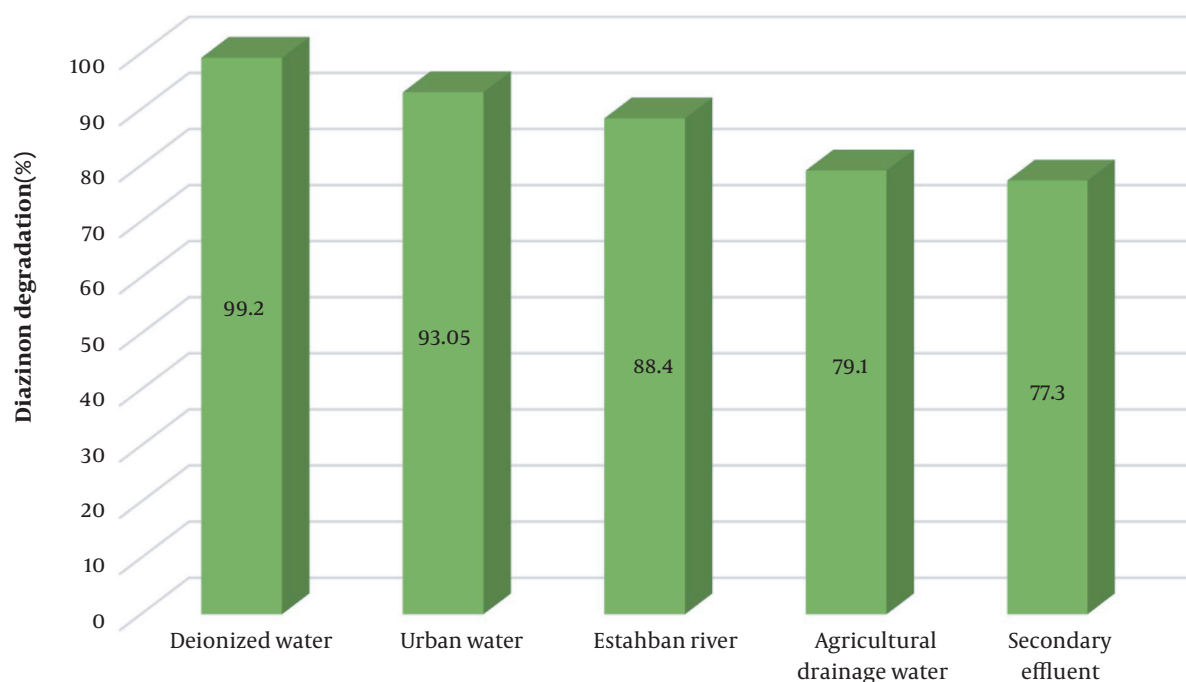


Figure 4. Efficiency of KMPS/MNPs/ozone system in actual environments (pH = 7, 0.6 g/L KMPS, 6 mg/L ozone, 0.1 g/L catalyst in 20 min).

Footnotes

Authors' Contribution: Study concept and design: Neematollah Jaafarzadeh and Taebeh Tabatabaie. Analysis and interpretation of data: Abdolrahim Pazira and Sahand Jorfi. Drafting of the manuscript: Seyed Jamshid Moosavi. Critical revision of the manuscript for important intellectual content: Neematollah Jaafarzadeh, Seyed Jamshid Moosavi, and Taebeh Tabatabaie. Statistical analysis: Abdolrahim Pazira.

Conflict of Interests: There is no conflict of interests.

Ethical Approval: Thesis code 162350421

Funding/Support: No fund was received.

References

- Talebi Jahromi K. [Pesticides toxicology]. Tehran, Iran: University of Tehran Press; 2013. Persian.
- Zhang Y, Pagilla K. Treatment of malathion pesticide wastewater with nanofiltration and photo-Fenton oxidation. *Desalination*. 2010;**263**(1-3):36-44. doi: [10.1016/j.desal.2010.06.031](https://doi.org/10.1016/j.desal.2010.06.031).
- Fadaei A, Dehghani MH, Nasser S, Mahvi AH, Rastkari N, Shayeghi M. Organophosphorous pesticides in surface water of Iran. *Bull Environ Contam Toxicol*. 2012;**88**(6):867-9. doi: [10.1007/s00128-012-0568-0](https://doi.org/10.1007/s00128-012-0568-0). [PubMed: [22349309](https://pubmed.ncbi.nlm.nih.gov/22349309/)].
- Dutta HM, Misquitta D, Khan S. The effects of endosulfan on the testes of bluegill fish, *Lepomis macrochirus*: a histopathological study. *Arch Environ Contam Toxicol*. 2006;**51**(1):149-56. doi: [10.1007/s00244-005-1061-0](https://doi.org/10.1007/s00244-005-1061-0). [PubMed: [16485171](https://pubmed.ncbi.nlm.nih.gov/16485171/)].
- Karataş A, Bahçeci Z. Toxic effects of diazinon on adult individuals of *Drosophila melanogaster*. *J. Appl. Biol. Sci.* 2009;**3**(2):111-7.
- Moudgil P, Gupta A, Sharma A, Gupta S, Tiwary AK. Potentiation of spermicidal activity of 2', 4'-dichlorobenzamil by lidocaine. *Indian J. Exp. Biol.* 2002;**40**(12):1373-7.
- Sarabia L, Maurer I, Bustos-Obregon E. Melatonin prevents damage elicited by the organophosphorous pesticide diazinon on the mouse testis. *Ecotoxicol Environ Saf.* 2009;**72**(3):938-42. doi: [10.1016/j.ecoenv.2008.04.022](https://doi.org/10.1016/j.ecoenv.2008.04.022). [PubMed: [18565581](https://pubmed.ncbi.nlm.nih.gov/18565581/)].
- Yousef MI, El-Demerdash FM, Al-Salhen KS. Protective role of isoflavones against the toxic effect of cypermethrin on semen quality and testosterone levels of rabbits. *J Environ Sci Health B*. 2003;**38**(4):463-78. doi: [10.1081/PFC-120021666](https://doi.org/10.1081/PFC-120021666). [PubMed: [12856928](https://pubmed.ncbi.nlm.nih.gov/12856928/)].
- Tang Y, Luo S, Teng Y, Liu C, Xu X, Zhang X, et al. Efficient removal of herbicide 2,4-dichlorophenoxyacetic acid from water using Ag/reduced graphene oxide co-decorated TiO₂ nanotube arrays. *J Hazard Mater*. 2012;**241-242**:323-30. doi: [10.1016/j.jhazmat.2012.09.050](https://doi.org/10.1016/j.jhazmat.2012.09.050). [PubMed: [23062512](https://pubmed.ncbi.nlm.nih.gov/23062512/)].
- Asgari G, Seidmohammadi A, Esrafil A, Faradmal J, Noori Sepehr M, Jafarinia M. The catalytic ozonation of diazinon using nano-MgO@CNT@Gr as a new heterogeneous catalyst: the optimization of effective factors by response surface methodology. *RSC Adv*. 2020;**10**(13):7718-31. doi: [10.1039/c9ra10095d](https://doi.org/10.1039/c9ra10095d).
- Khoiriah K, Wellia DV, Gunlazuardi J, Safni S. Photocatalytic Degradation of Commercial Diazinon Pesticide Using C,N-codoped TiO₂ as Photocatalyst. *Indones. J. Chem.* 2020;**20**(3):587-96. doi: [10.22146/ijc.43982](https://doi.org/10.22146/ijc.43982).

12. Molla Mahmoudi M, Khaghani R, Dargahi A, Monazami Tehrani G. Electrochemical degradation of diazinon from aqueous media using graphite anode: Effect of parameters, mineralisation, reaction kinetic, degradation pathway and optimisation using central composite design. *Int J Environ Anal Chem.* 2020;1-26. doi: [10.1080/03067319.2020.1742893](https://doi.org/10.1080/03067319.2020.1742893).
13. Heidari M, Vosoughi M, Sadeghi H, Dargahi A, Mokhtari SA. Degradation of diazinon from aqueous solutions by electro-Fenton process: effect of operating parameters, intermediate identification, degradation pathway, and optimization using response surface methodology (RSM). *Sep Sci Technol.* 2021;56(13):2287-99. doi: [10.1080/01496395.2020.1821060](https://doi.org/10.1080/01496395.2020.1821060).
14. Farhadi S, Sohrabi MR, Motiee F, Davallo M. Organophosphorus diazinon pesticide removing from aqueous solution by zero-valent iron supported on biopolymer chitosan: RSM optimization methodology. *J Polym Environ.* 2021;29(1):103-20.
15. Glaze WH, Kang JW, Chapin DH. The Chemistry of Water Treatment Processes Involving Ozone, Hydrogen Peroxide and Ultraviolet Radiation. *Ozone Sci Eng.* 1987;9(4):335-52. doi: [10.1080/01919518708552148](https://doi.org/10.1080/01919518708552148).
16. Brillas E, Sires I, Oturan MA. Electro-Fenton process and related electrochemical technologies based on Fenton's reaction chemistry. *Chem Rev.* 2009;109(12):6570-631. doi: [10.1021/cr900136g](https://doi.org/10.1021/cr900136g). [PubMed: 19839579].
17. Nidheesh PV, Gandhimathi R, Ramesh ST. Degradation of dyes from aqueous solution by Fenton processes: a review. *Environ Sci Pollut Res Int.* 2013;20(4):2099-132. doi: [10.1007/s11356-012-1385-z](https://doi.org/10.1007/s11356-012-1385-z). [PubMed: 23338990].
18. Vilhunen S, Sillanpää M. Recent developments in photochemical and chemical AOPs in water treatment: a mini-review. *Rev Environ. Sci. Biotechnol.* 2010;9(4):323-30. doi: [10.1007/s1157-010-9216-5](https://doi.org/10.1007/s1157-010-9216-5).
19. Asghar A, Abdul Raman AA, Wan Daud WMA. Advanced oxidation processes for in-situ production of hydrogen peroxide/hydroxyl radical for textile wastewater treatment: a review. *J. Clean. Prod.* 2015;87:826-38. doi: [10.1016/j.jclepro.2014.09.010](https://doi.org/10.1016/j.jclepro.2014.09.010).
20. Buxton GV, Greenstock CL, Helman WP, Ross AB. Critical Review of rate constants for reactions of hydrated electrons, hydrogen atoms and hydroxyl radicals ($\cdot\text{OH}/\cdot\text{O}-$ in Aqueous Solution). *J Phys Chem Ref Data.* 1988;17(2):513-886. doi: [10.1063/1.555805](https://doi.org/10.1063/1.555805).
21. Anipsitakis GP, Dionysiou DD. Degradation of organic contaminants in water with sulfate radicals generated by the conjunction of peroxy-monosulfate with cobalt. *Environ Sci Technol.* 2003;37(20):4790-7. doi: [10.1021/es0263792](https://doi.org/10.1021/es0263792). [PubMed: 14594393].
22. Ghanbari F, Moradi M, Manshouri M. Textile wastewater decolorization by zero valent iron activated peroxy-monosulfate: Compared with zero valent copper. *J. Environ. Chem. Eng.* 2014;2(3):1846-51. doi: [10.1016/j.jece.2014.08.003](https://doi.org/10.1016/j.jece.2014.08.003).
23. Lin H, Wu J, Zhang H. Degradation of bisphenol A in aqueous solution by a novel electro/Fe³⁺/peroxydisulfate process. *Sep. Purif. Technol.* 2013;117:18-23. doi: [10.1016/j.seppur.2013.04.026](https://doi.org/10.1016/j.seppur.2013.04.026).
24. Olmez-Hanci T, Arslan-Alaton I. Comparison of sulfate and hydroxyl radical based advanced oxidation of phenol. *Chem. Eng. J.* 2013;224:10-6. doi: [10.1016/j.cej.2012.11.007](https://doi.org/10.1016/j.cej.2012.11.007).
25. Jaafarzadeh N, Ghanbari F, Moradi M. Photo-electro-oxidation assisted peroxy-monosulfate for decolorization of acid brown 14 from aqueous solution. *Korean J Chem Eng.* 2015;32(3):458-64. doi: [10.1007/s11814-014-0263-4](https://doi.org/10.1007/s11814-014-0263-4).
26. Tan C, Gao N, Deng Y, Rong W, Zhou S, Lu N. Degradation of antipyrine by heat activated persulfate. *Sep. Purif. Technol.* 2013;109:122-8. doi: [10.1016/j.seppur.2013.03.003](https://doi.org/10.1016/j.seppur.2013.03.003).
27. Anipsitakis GP, Dionysiou DD. Radical generation by the interaction of transition metals with common oxidants. *Environ Sci Technol.* 2004;38(13):3705-12. doi: [10.1021/es035121o](https://doi.org/10.1021/es035121o). [PubMed: 15296324].
28. Ghanbari F, Moradi M. Application of peroxy-monosulfate and its activation methods for degradation of environmental organic pollutants: Review. *Chem. Eng. J.* 2017;310:41-62. doi: [10.1016/j.cej.2016.10.064](https://doi.org/10.1016/j.cej.2016.10.064).
29. Hu P, Long M. Cobalt-catalyzed sulfate radical-based advanced oxidation: A review on heterogeneous catalysts and applications. *Appl. Catal. B.* 2016;181:103-17. doi: [10.1016/j.apcatb.2015.07.024](https://doi.org/10.1016/j.apcatb.2015.07.024).
30. Oh WD, Dong Z, Lim T. Generation of sulfate radical through heterogeneous catalysis for organic contaminants removal: Current development, challenges and prospects. *Appl. Catal. B.* 2016;194:169-201. doi: [10.1016/j.apcatb.2016.04.003](https://doi.org/10.1016/j.apcatb.2016.04.003).
31. Guan YH, Ma J, Ren YM, Liu YL, Xiao JY, Lin LQ, et al. Efficient degradation of atrazine by magnetic porous copper ferrite catalyzed peroxy-monosulfate oxidation via the formation of hydroxyl and sulfate radicals. *Water Res.* 2013;47(14):5431-8. doi: [10.1016/j.watres.2013.06.023](https://doi.org/10.1016/j.watres.2013.06.023). [PubMed: 23916710].
32. Chandran HT, Thangavel S, Jipsa CV, Venugopal G. Study on inorganic oxidants assisted sonocatalytic degradation of Resazurin dye in presence of β -SnWO₄ nanoparticles. *Mater Sci Semicond Process.* 2014;27:212-9. doi: [10.1016/j.mssp.2014.06.021](https://doi.org/10.1016/j.mssp.2014.06.021).
33. Cheng X, Liang H, Ding A, Tang X, Liu B, Zhu X, et al. Ferrous iron/peroxy-monosulfate oxidation as a pretreatment for ceramic ultrafiltration membrane: Control of natural organic matter fouling and degradation of atrazine. *Water Res.* 2017;113:32-41. doi: [10.1016/j.watres.2017.01.055](https://doi.org/10.1016/j.watres.2017.01.055). [PubMed: 28187348].
34. Zhang BT, Zhang Y, Teng Y, Fan M. Sulfate Radical and Its Application in Decontamination Technologies. *Crit Rev Environ Sci Technol.* 2015;45(16):1756-800. doi: [10.1080/10643389.2014.970681](https://doi.org/10.1080/10643389.2014.970681).
35. Hai FI, Yamamoto K, Fukushi K. Hybrid Treatment Systems for Dye Wastewater. *Crit Rev Environ Sci Technol.* 2007;37(4):315-77. doi: [10.1080/10643380601174723](https://doi.org/10.1080/10643380601174723).
36. Pignatello JJ, Oliveros E, MacKay A. Advanced Oxidation Processes for Organic Contaminant Destruction Based on the Fenton Reaction and Related Chemistry. *Crit Rev Environ Sci Technol.* 2006;36(1):1-84. doi: [10.1080/10643380500326564](https://doi.org/10.1080/10643380500326564).
37. Munoz M, de Pedro ZM, Casas JA, Rodriguez JJ. Preparation of magnetite-based catalysts and their application in heterogeneous Fenton oxidation - A review. *Appl. Catal. B.* 2015;176-177:249-65. doi: [10.1016/j.apcatb.2015.04.003](https://doi.org/10.1016/j.apcatb.2015.04.003).
38. He J, Yang X, Men B, Wang D. Interfacial mechanisms of heterogeneous Fenton reactions catalyzed by iron-based materials: A review. *J Environ Sci (China).* 2016;39:97-109. doi: [10.1016/j.jes.2015.12.003](https://doi.org/10.1016/j.jes.2015.12.003). [PubMed: 26899649].
39. Wan D, Li W, Wang G, Lu L, Wei X. Degradation of p-Nitrophenol using magnetic Fe(0)/Fe₃O₄/Coke composite as a heterogeneous Fenton-like catalyst. *Sci Total Environ.* 2017;574:1326-34. doi: [10.1016/j.scitotenv.2016.08.042](https://doi.org/10.1016/j.scitotenv.2016.08.042). [PubMed: 27519319].
40. Dang HT, Nguyen T, Nguyen T, Thi SQ, Tran HT, Tran HQ, et al. Magnetic CuFe₂O₄ Prepared by Polymeric Precursor Method as a Reusable Heterogeneous Fenton-like Catalyst for the Efficient Removal of Methylene Blue. *Chem Eng Commun.* 2016;203(9):1260-8. doi: [10.1080/00986445.2016.1174858](https://doi.org/10.1080/00986445.2016.1174858).
41. Garg VK, Sharma VK, Kuzmann E. Purification of Water by Ferrites - Mini Review. *Ferrites and Ferrates: Chemistry and Applications in Sustainable Energy and Environmental Remediation.* 1238. Washington, D.C., USA: American Chemical Society; 2016. p. 137-43. doi: [10.1021/bk-2016-1238.ch005](https://doi.org/10.1021/bk-2016-1238.ch005).
42. Zhang T, Zhu H, Croue JP. Production of sulfate radical from peroxy-monosulfate induced by a magnetically separable CuFe₂O₄ spinel in water: efficiency, stability, and mechanism. *Environ Sci Technol.* 2013;47(6):2784-91. doi: [10.1021/es304721g](https://doi.org/10.1021/es304721g). [PubMed: 23439015].
43. Zou L, Wang Q, Shen X, Wang Z, Jing M, Luo Z. Fabrication and dye removal performance of magnetic CuFe₂O₄@CeO₂ nanofibers. *Appl.*

- Surf. Sci. 2015;**332**:674–81. doi: [10.1016/j.apsusc.2015.01.176](https://doi.org/10.1016/j.apsusc.2015.01.176).
44. Zhang X, Feng M, Qu R, Liu H, Wang L, Wang Z. Catalytic degradation of diethyl phthalate in aqueous solution by persulfate activated with nano-scaled magnetic CuFe₂O₄/MWCNTs. *Chem. Eng. J.* 2016;**301**:1–11. doi: [10.1016/j.cej.2016.04.096](https://doi.org/10.1016/j.cej.2016.04.096).
 45. Qi F, Chu W, Xu B. Ozonation of phenacetin in associated with a magnetic catalyst CuFe₂O₄: The reaction and transformation. *Chem. Eng. J.* 2015;**262**:552–62. doi: [10.1016/j.cej.2014.09.068](https://doi.org/10.1016/j.cej.2014.09.068).
 46. Mahmoodi NM. Photocatalytic ozonation of dyes using copper ferrite nanoparticle prepared by co-precipitation method. *Desalination*. 2011;**279**(1):332–7. doi: [10.1016/j.desal.2011.06.027](https://doi.org/10.1016/j.desal.2011.06.027).
 47. Moosavia SJ, Paziraa A, Tabatabaiea T, Jaafarzadeha N, Jorfia S. Determining diazinon degradation using potassium hydrogen monopersulfate and magnetic copper ferrite nano-particles in contact with ozone in aqueous solutions. *Desalination Water Treat.* 2021;**216**:263–82.
 48. Jeffery GH. *Vogel's Textbook of Quantitative Chemical Analysis*. 5 ed. London, England: Longman Scientific & Technical; 1989. 877 p.
 49. Clesceri LS, Greenberg AE, Eaton AD. *Standard Methods for the Examination of Water and Wastewater, 20th Edition*. Washington, D.C., USA: APHA American Public Health Association; 1998.
 50. Jung YS, Lim WT, Park JY, Kim YH. Effect of pH on Fenton and Fenton-like oxidation. *Environ Technol.* 2009;**30**(2):183–90. doi: [10.1080/09593330802468848](https://doi.org/10.1080/09593330802468848). [PubMed: [19278159](https://pubmed.ncbi.nlm.nih.gov/19278159/)].
 51. Chen Q, Ji F, Liu T, Yan P, Guan W, Xu X. Synergistic effect of bifunctional Co-TiO₂ catalyst on degradation of Rhodamine B: Fenton-photo hybrid process. *Chem. Eng. J.* 2013;**229**:57–65. doi: [10.1016/j.cej.2013.04.024](https://doi.org/10.1016/j.cej.2013.04.024).
 52. Yang N, Cui J, Zhang L, Xiao W, Alshawabkeh AN, Mao X. Iron electrolysis-assisted peroxymonosulfate chemical oxidation for the remediation of chlorophenol-contaminated groundwater. *J Chem Technol Biotechnol.* 2016;**91**(4):938–47. doi: [10.1002/jctb.4659](https://doi.org/10.1002/jctb.4659). [PubMed: [30473593](https://pubmed.ncbi.nlm.nih.gov/30473593/)]. [PubMed Central: [PMC6247945](https://pubmed.ncbi.nlm.nih.gov/PMC6247945/)].
 53. Ghanbari F, Moradi M. *Electrooxidation processes for dye degradation and colored wastewater treatment*. London, United Kingdom: CRC Press LLC, London; 2016.
 54. Huang YH, Huang YF, Huang CI, Chen CY. Efficient decolorization of azo dye Reactive Black B involving aromatic fragment degradation in buffered Co²⁺/PMS oxidative processes with a ppb level dosage of Co²⁺-catalyst. *J Hazard Mater.* 2009;**170**(2-3):1110–8. doi: [10.1016/j.jhazmat.2009.05.091](https://doi.org/10.1016/j.jhazmat.2009.05.091). [PubMed: [19541412](https://pubmed.ncbi.nlm.nih.gov/19541412/)].
 55. Sun J, Song M, Feng J, Pi Y. Highly efficient degradation of ofloxacin by UV/Oxone/Co²⁺ oxidation process. *Environ Sci Pollut Res Int.* 2012;**19**(5):1536–43. doi: [10.1007/s11356-011-0654-6](https://doi.org/10.1007/s11356-011-0654-6). [PubMed: [22072118](https://pubmed.ncbi.nlm.nih.gov/22072118/)].
 56. Sun JH, Sun SP, Sun JY, Sun RX, Qiao LP, Guo HQ, et al. Degradation of azo dye Acid black 1 using low concentration iron of Fenton process facilitated by ultrasonic irradiation. *Ultrason Sonochem.* 2007;**14**(6):761–6. doi: [10.1016/j.ultsonch.2006.12.010](https://doi.org/10.1016/j.ultsonch.2006.12.010). [PubMed: [17291814](https://pubmed.ncbi.nlm.nih.gov/17291814/)].
 57. Guo L, Zhong Q, Ding J, Ou M, Lv Z, Song F. Low-Temperature NO_x (x = 1, 2) Removal with •OH Radicals from Catalytic Ozonation over α-FeOOH. *Ozone Sci Eng.* 2016;**38**(5):382–94. doi: [10.1080/01919512.2016.1198685](https://doi.org/10.1080/01919512.2016.1198685).
 58. Ling SK, Wang S, Peng Y. Oxidative degradation of dyes in water using Co²⁺/H₂O₂ and Co²⁺/peroxymonosulfate. *J Hazard Mater.* 2010;**178**(1-3):385–9. doi: [10.1016/j.jhazmat.2010.01.091](https://doi.org/10.1016/j.jhazmat.2010.01.091). [PubMed: [20144502](https://pubmed.ncbi.nlm.nih.gov/20144502/)].
 59. Madhavan J, Maruthamuthu P, Murugesan S, Ashokkumar M. Kinetics of degradation of acid red 88 in the presence of Co²⁺/ion/peroxomonosulphate reagent. *APPL CATAL A-GEN.* 2009;**368**(1):35–9. doi: [10.1016/j.apcata.2009.08.008](https://doi.org/10.1016/j.apcata.2009.08.008).
 60. Madhavan J, Muthuraaman B, Murugesan S, Anandan S, Maruthamuthu P. Peroxomonosulphate, an efficient oxidant for the photocatalysed degradation of a textile dye, acid red 88. *Sol. Energy Mater Sol. Cells.* 2006;**90**(13):1875–87. doi: [10.1016/j.solmat.2005.12.001](https://doi.org/10.1016/j.solmat.2005.12.001).
 61. Yang Y, Jiang J, Lu X, Ma J, Liu Y. Production of sulfate radical and hydroxyl radical by reaction of ozone with peroxymonosulfate: a novel advanced oxidation process. *Environ Sci Technol.* 2015;**49**(12):7330–9. doi: [10.1021/es506362e](https://doi.org/10.1021/es506362e). [PubMed: [25988821](https://pubmed.ncbi.nlm.nih.gov/25988821/)].
 62. Zeng T, Zhang X, Wang S, Niu H, Cai Y. Spatial confinement of a Co₃O₄ catalyst in hollow metal-organic frameworks as a nanoreactor for improved degradation of organic pollutants. *Environ Sci Technol.* 2015;**49**(4):2350–7. doi: [10.1021/es505014z](https://doi.org/10.1021/es505014z). [PubMed: [25608052](https://pubmed.ncbi.nlm.nih.gov/25608052/)].
 63. Wang Y, Xie Y, Sun H, Xiao J, Cao H, Wang S. Hierarchical shape-controlled mixed-valence calcium manganites for catalytic ozonation of aqueous phenolic compounds. *Catal. Sci. Technol.* 2016;**6**(9):2918–29. doi: [10.1039/c5cy01967b](https://doi.org/10.1039/c5cy01967b).
 64. Zhou Y, Jiang J, Gao Y, Ma J, Pang SY, Li J, et al. Activation of Peroxymonosulfate by Benzoquinone: A Novel Nonradical Oxidation Process. *Environ Sci Technol.* 2015;**49**(12):12941–50. doi: [10.1021/acs.est.5b03595](https://doi.org/10.1021/acs.est.5b03595). [PubMed: [26452059](https://pubmed.ncbi.nlm.nih.gov/26452059/)].
 65. Qi C, Liu X, Ma J, Lin C, Li X, Zhang H. Activation of peroxymonosulfate by base: Implications for the degradation of organic pollutants. *Chemosphere.* 2016;**151**:280–8. doi: [10.1016/j.chemosphere.2016.02.089](https://doi.org/10.1016/j.chemosphere.2016.02.089). [PubMed: [26946115](https://pubmed.ncbi.nlm.nih.gov/26946115/)].
 66. Wang Y, Xie Y, Sun H, Xiao J, Cao H, Wang S. Efficient Catalytic Ozonation over Reduced Graphene Oxide for p-Hydroxybenzoic Acid (PHBA) Destruction: Active Site and Mechanism. *ACS Appl Mater Interfaces.* 2016;**8**(15):9710–20. doi: [10.1021/acsami.6b01175](https://doi.org/10.1021/acsami.6b01175). [PubMed: [27007603](https://pubmed.ncbi.nlm.nih.gov/27007603/)].
 67. Ahmadi M, Ghanbari F, Moradi M. Photocatalysis assisted by peroxymonosulfate and persulfate for benzotriazole degradation: effect of pH on sulfate and hydroxyl radicals. *Water Sci Technol.* 2015;**72**(11):2095–102. doi: [10.2166/wst.2015.437](https://doi.org/10.2166/wst.2015.437). [PubMed: [26606105](https://pubmed.ncbi.nlm.nih.gov/26606105/)].
 68. Yao Y, Cai Y, Lu F, Wei F, Wang X, Wang S. Magnetic recoverable MnFe(2)O(4) and MnFe(2)O(4)-graphene hybrid as heterogeneous catalysts of peroxymonosulfate activation for efficient degradation of aqueous organic pollutants. *J Hazard Mater.* 2014;**270**:61–70. doi: [10.1016/j.jhazmat.2014.01.027](https://doi.org/10.1016/j.jhazmat.2014.01.027). [PubMed: [24548886](https://pubmed.ncbi.nlm.nih.gov/24548886/)].
 69. Wang Y, Xie Y, Sun H, Xiao J, Cao H, Wang S. 2D/2D nano-hybrids of γ-MnO₂ on reduced graphene oxide for catalytic ozonation and coupling peroxymonosulfate activation. *Journal of Hazardous Materials.* 2016;**301**:56–64. doi: [10.1016/j.jhazmat.2015.08.031](https://doi.org/10.1016/j.jhazmat.2015.08.031).